

## Research Paper

# Mutually Orthogonal Golay Complementary Sequences in Medical Ultrasound Diagnostics. Experimental Study

Ihor TROTS\*, Norbert ŻOLEK, Yuriy TASINKEVYCH, Janusz WÓJCIK

*Ultrasound Department  
Institute of Fundamental Technological Research, Polish Academy of Sciences  
Warsaw, Poland*

\*Corresponding Author e-mail: igortr@ippt.pan.pl

(received October 5, 2021; accepted May 26, 2022)

The objective of this paper is an experimental study of the most crucial parameters of the received acoustic signals (e.g. signal-to-noise ratio (SNR), side-lobes level (SLL), axial resolution) obtained as a result of simultaneous emission of mutually orthogonal Golay complementary sequences (MOGCS) to demonstrate their feasibility of being used in ultrasound diagnostics. Application of the MOGCS in ultrasound measurements allows the image reconstruction time to be shortened without decreasing the resulting quality of reconstructed images in comparison with regular complementary Golay coded sequences (CGCS). In this paper two sets of 16-bits long MOGCS were implemented in the Verasonics Vantage<sup>TM</sup> (Verasonics Inc., Kirkland, WA, USA) scanner. Ultrasound data were generated using a perfect reflector, a custom-made nylon wire phantom and tissue mimicking phantom. Parameters of the detected MOGCS echoes like SNR, SLL and axial resolution were determined and compared to that of the standard CGCS and the short two-sine cycles pulse. It was evidenced that applying MOGCS did not compromise the parameters of the separated and compressed echoes in comparison to the other types of transmitted signal – the CGCS and the short pulse. Concretely, both the MOGCS and CGCS yield similar SNR increase in comparison to the short pulse. Almost similar values of the axial resolution estimated at the full width at the half maximum level for all types of the transmitted signals were also obtained. At the same time, using the MOGCS the data acquisition speed can be increased twice in comparison with the CGCS signal.

**Keywords:** coded excitation; mutually orthogonal Golay codes; synthetic aperture; ultrasound imaging.



Copyright © 2022 I. Trots *et al.*  
This is an open-access article distributed under the terms of the Creative Commons Attribution-ShareAlike 4.0 International (CC BY-SA 4.0 <https://creativecommons.org/licenses/by-sa/4.0/>) which permits use, distribution, and reproduction in any medium, provided that the article is properly cited, the use is non-commercial, and no modifications or adaptations are made.

## 1. Introduction

In ultrasound diagnostics image requirements are becoming more and more demanding. Penetration depth, signal-to-noise ratio (SNR), high resolution image are the most important parameters in modern ultrasound diagnostics. The SNR and penetration depth depend on the energy dissipation due to the propagating acoustic wave attenuation in the medium. The high-peak transmit power is strictly regulated by medical standards (IEC 60601-2-37). It limits the possibility of the increase of SNR and penetration depth by amplifying the transmitted signal power. On the other hand, the axial and lateral ultrasound image resolutions depend on the frequency of transmitted signal and the beam width which is a function of the transmitted

wavelength and the aperture size. It is known that for higher frequencies of the transmitted signal attenuation increases, and this effect is particularly noticeable at greater depths. To overcome this difficulty the wide-band transmitting signals, or the so-called coded sequences, combined with compression techniques of the received echoes can be applied (NOWICKI *et al.*, 2003). The average transmitted power is proportional to the code length. Coding of the transmitted signal and compression of the received echoes allows increasing the SNR and visualization depth without amplifying the transmitted signal (TROTS *et al.*, 2011). This also allows the transmit frequency to be increased. Among different excitation sequences proposed in ultrasonography, Golay codes have been receiving growing attention in comparison with other signals. This

is due to their unique property which is the suppression of side-lobes influence in the signal. This type of codes was first introduced by GOLAY (1961) and is also known as complementary Golay coded sequences (CGCS). A detailed discussion on the construction and properties of the sequences as well as compression techniques based on correlation of the received signals with transmitted waveforms are described in (TROTS *et al.*, 2004).

Another crucial factor in ultrasound medical imaging diagnostics is the frame rate or the speed of image reconstruction defined as a number of reconstructed images frames per second (FPS). Apart from computational speed related to the image reconstruction algorithm implementation and the hardware used, it is physically limited by the speed of data acquisition, which depends on the acoustic wave speed in the medium, depth of visualization and the number of imaging lines. One possible solution to this problem is simultaneous transmission of several interrogation signals. The corresponding echoes must then be separated in reception yielding several frames reconstructed in parallel. Efficient separation of echoes resulting from different transmitted signals is only possible if the signals are orthogonal. Fortunately, it appears that among different Golay coded sequences it is possible to find complementary pairs which at the same time are orthogonal. Such sequences are known as mutually orthogonal Golay complementary sequences (MOGCS) (BAE, 2003). Mutually orthogonal complementary sets (MOCS) have received significant research attention in recent years due to their wide applications not only in ultrasonography but in communications and radars. For this reason, MOCS are gaining more and more interest (WU *et al.*, 2021; TIAN *et al.*, 2021). Orthogonality of MOGCS means that the sum of cross-correlation functions for corresponding sequences in two MOGCS is zero. Applying the MOGCS the acoustic data acquisition and, as a result, the frame rate of the image reconstruction can be increased significantly. Several ultrasound imaging approaches based on application of the MOGCS were reported in the literature (CHIAO, THOMAS, 2000; BAE *et al.*, 2002; KIM, SONG, 2003; PENG *et al.*, 2006; ZHAO, LUO, 2018; KUMRU, KOYMEN, 2018). All above mention works are mainly focused on 2D B-mode image reconstruction and comparison of two sets of MOGCS simultaneous transmission with short pulse transmission. However, no profound analysis of the MOGCS echoes proving the efficiency of match filtering in the case of experimentally obtained data was reported in the literature so far.

The goal of this work is an experimental study of the received acoustic signals obtained as a result of simultaneous emission of different MOGCS sets to demonstrate their feasibility of being used in ultrasound diagnostics. For this purpose the acoustic echoes from a brass plate modelling a perfect reflector,

from a custom-made nylon wire phantom and tissue-mimicking phantom (model 525 Danish Phantom Design) were measured, analyzed and compared for different excitation signals. Specifically, the parameters of the received signals, obtained as a result of simultaneous transmission of two 16-bits long sets of MOGCS were compared with conventional CGCS and the short two-sine cycles pulse excitation was conducted. Such parameters like the pulse duration estimated at the  $-6$  dB and  $-20$  dB level, signal SLL and the SNR were estimated for the above three types of transmitted signals. In the case of the MOGCS and CGSC emissions the received signals were processed with matched filters in order to separate the echoes and compress them to suppress the signal side-lobes. The experimental measurements were carried out using commercial ultrasound system Verasonics Vantage<sup>TM</sup> (Verasonics Inc., Kirkland, WA, USA) equipped with a linear 128-element probe L7-7.

## 2. Method

Conventional pair of the 16-bits CGCS, two 16-bits long MOGCS sets and two-sine cycle pulse (short pulse) at a nominal frequency of 5 MHz were generated by the Verasonics Vantage<sup>TM</sup> research ultrasound system using the 128 element linear ultrasound transducer L7-4.

The block diagram of the experimental setup is shown in Fig. 1.

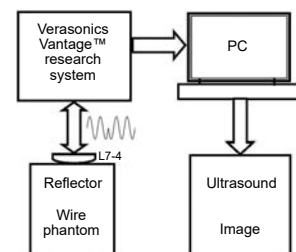


Fig. 1. Block diagram of the experimental setup.

First, the ultrasound echoes were collected using a perfect reflector immersed in a water tank. The signals obtained from the reflector allowed estimation of the compressed pulse duration for MOGCS, CGCS and the short pulse excitation. Next, the measurements were repeated with a custom-made wire phantom. The phantom consisted of fine nylon wires ( $\varnothing 0.06$  mm). There were 22 wires arranged vertically and spaced 2 mm axially. The signals collected from the wire phantom allowed comparison of the SLL for different types of excitation. Finally, to compare the SNR for different signals the experiments were carried out for a tissue mimicking phantom (model 525 Danish Phantom Design) with attenuation  $0.5$  dB/(MHz · cm).

To gain an insight into the MOGCS data processing algorithm, it might be appropriate to consider the

data acquisition scheme shown in Fig. 2. This diagram depicts the approach, in which two MOGCS sets,  $A_i$  and  $B_i$ , are transmitted by two neighbouring elements of a linear array transducer. Specifically, the transducer array element #1 transmits the code  $A_1$  and the element #2 transmits the code  $B_1$  during the first transmission of MOGCS sets. Next, the element #1 transmits the code  $A_2$  and the element #2 transmits the code  $B_2$  during the second transmission. In both transmit events the ultrasound echoes are acquired simultaneously by all elements of the transducer array. In the case of CGCS only one complementary pair is transmitted by the element #1. It means that during the first transmission the element #1 transmits the code  $A_1$  and during the second transmission the element #1 transmits the code  $B_1$ . In this paper only one code from two sequences (code  $A_1$ ) was compared and analyzed assuming that the compressed echo from the second code is identical to the first with the difference that the side-lobes are in the opposite phase (TROTS *et al.*, 2004). The short pulse was transmitted and received by the element #1 as well. Raw data were collected with sampling rate of 25 MHz and stored in the memory for further processing. Recorded echoes resulting from MOGCS transmission were processed as discussed in the Sec. 3. The CGCS echoes were processed using conventional matched filtering technique in order to compress recorded signals and suppress the side-lobes (MISARIDIS, 2001). The signal processing algorithms mentioned above were implemented in MATLAB<sup>®</sup>.

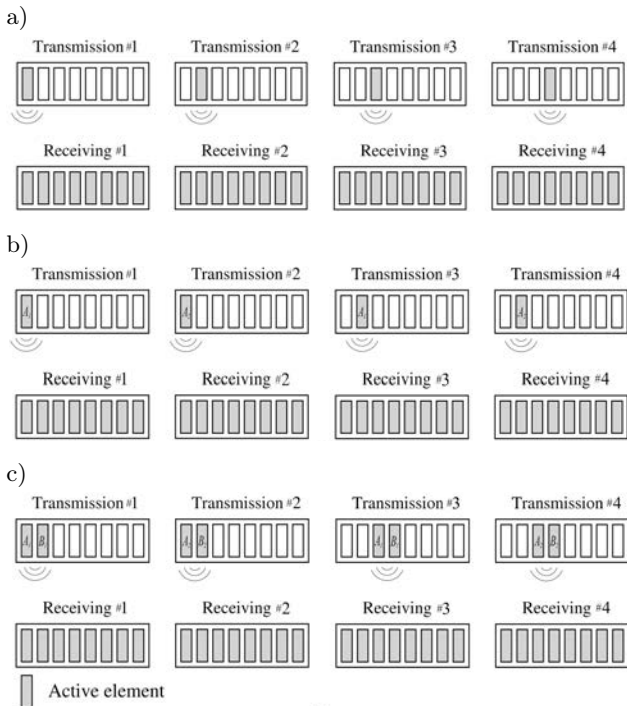


Fig. 2. Transmission and receiving method using conventional STA method (a); the CGCS in STA method (b); the MOGCS in STA method for  $M = 2$  (c).

### 3. Theory

The main advantage of the CGCS is that they allow the side-lobes to be suppressed yielding significant improvement of the SNR over the short pulse excitation (1–2 cycles of operating frequency) (TROTS *et al.*, 2004). In contrast to the short pulse excitation, the CGCS requires two consecutive transmissions to generate a single scan line of the image. This means that data acquisition lasts two times longer for the CGCS in comparison to the short pulse excitation. This drawback can successfully be overcome by applying the MOGCS. The MOGCS are essentially different pairs of CGCS possessing the mutual orthogonality property (BAE, 2003). It allows two or more different complementary pairs of CGCS to be transmitted simultaneously without interfering with each other. As a result two image lines can be constructed after two transmissions. In this work the 2-order mutually orthogonal set was used. If the 4- or 8-order mutually orthogonal set will be used, the 4 or 8 image lines can be constructed after two transmissions. This principle was described in details in the work (TROTS, 2015; TROTS *et al.*, 2015). This enables increasing the data acquisition rate in comparison with the CGCS or even with the short pulse, if more than two MOGCS sets are used simultaneously (TROTS *et al.*, 2004). On reception the echoes corresponding to simultaneously transmitted MOGCS can be separated using Golay codes compression algorithm, briefly presented below. Specifically, consider a set of  $L$ -bits long codes  $A_i$  and  $B_i$ ,  $i = 1, 2, \dots, M$ , being a complementary pairs (i.e.  $A_1A_2$  is a complementary pair #1 and  $B_1B_2$  is a complementary pair #2) which obey the following condition (TROTS *et al.*, 2015):

$$R_{A_1}(n) + R_{A_2}(n) = \begin{cases} 2L, & n = 0, \\ 0, & n \neq 0, \end{cases} \quad (1)$$

$$R_{B_1}(n) + R_{B_2}(n) = \begin{cases} 2L, & n = 0, \\ 0, & n \neq 0, \end{cases}$$

where the autocorrelation function  $R$  of the coded sequence in Eq. (1) is defined as follows (MISARIDIS, 2001):

$$R(n) = \begin{cases} \sum_{k=0}^{L-1-n} S(k)S(k-n), & n = 0, \dots, L-1, \\ R(-n), & n = -(L-1), \dots, -1, \end{cases} \quad (2)$$

and  $S(k)$ ,  $k = 0, \dots, L-1$  denotes the coded sequence  $A_i$ ,  $B_i$ ,  $i = 1, 2$  of the length  $L$ . Furthermore, the two CGCS pairs  $A_i$  and  $B_i$  are said to be mutually orthogonal pairs, or MOGCS pairs, if the sum of the corresponding cross-correlation functions vanishes:

$$\sum_{i,j=1}^2 R_{A_i B_j} = 0. \quad (3)$$

The cross-correlation functions in Eq. (3) are defined as follows (TSENG, LIU, 1972):

$$R_{A_i B_j}(n) = \begin{cases} \sum_{k=0}^{L-1-n} A_i(k) B_j(k-n), & n = 0, \dots, L-1, \\ \sum_{k=0}^{L-1-n} A_i(k-n) B_j(k), & n = -(L-1), \dots, -1. \end{cases} \quad (4)$$

Thereby, the CGCS pairs  $A_i$  and  $B_i$ ,  $i = 1, 2$ , comprise the MOGCS set if they simultaneously obey Eqs (1) and (3). The main consequence of the mutual orthogonality, defined in Eq. (3), is the ability to transmit two CGCS pairs simultaneously without interfering in reception. The echoes corresponding to different CGCS pairs comprising the MOGCS set can be efficiently extracted from the received signal using Golay codes compression algorithm, briefly discussed below.

To illustrate this, consider the following example of 2 sets of MOGCS (similar codes were used in experimental measurements). Two orthogonal sets of  $\{A, B\}$  can be written as follows:

$$A_1 = [1 \ 11 \ -11 \ 1 \ -1 \ 1 \ 1 \ 1 \ 1 \ -1 \ -1 \ -1 \ 1 \ -1],$$

$$A_2 = [1 \ -11 \ 11 \ -1 \ -1 \ -1 \ 1 \ -1 \ 1 \ 1 \ -1 \ 1 \ 1 \ 1],$$

$$B_1 = [1 \ 11 \ -11 \ 1 \ -1 \ 1 \ -1 \ -1 \ -1 \ 1 \ 1 \ 1 \ -1 \ 1],$$

$$B_2 = [1 \ -11 \ 11 \ -1 \ -1 \ -1 \ -1 \ 1 \ -1 \ -1 \ 1 \ -1 \ -1 \ -1],$$

where the orthogonal Golay sequences of the length of  $L = 16$  bits were assumed. The two code sequences  $\{A_i, B_i\}$  are transmitted by two transducer elements  $\{\#1$  and  $\#2\}$ . Specifically the orthogonal signals  $\{A_1, B_1\}$  are transmitted first. Then, the corresponding echoes are detected and stored for further processing. Next, the process is repeated for the second pair of orthogonal signals  $\{A_2, B_2\}$ . The detected signals being a superposition of echoes corresponding to  $\{A_i, B_i\}$  can be compressed by adding together the correlation functions of each of the received sequences with the sequence transmitted by the same transducer element. For example, in order to recover the echo for transducer element  $\#1$  (i.e. the pair  $A_i$  that was transmitted by transducer element  $\#1$ ), for the first and second transmissions one should compute the sum of cross-correlation functions of the received signals  $S_i$  with corresponding transmitted codes  $A_i$ ,  $i = 1, 2$  using Eq. (3) as follows:

$$P_A = \sum_{i=1}^2 R_{S_i A_i}. \quad (5)$$

#### 4. Results and discussion

In Fig. 3 the RF echoes reflected from the perfect reflector are shown.

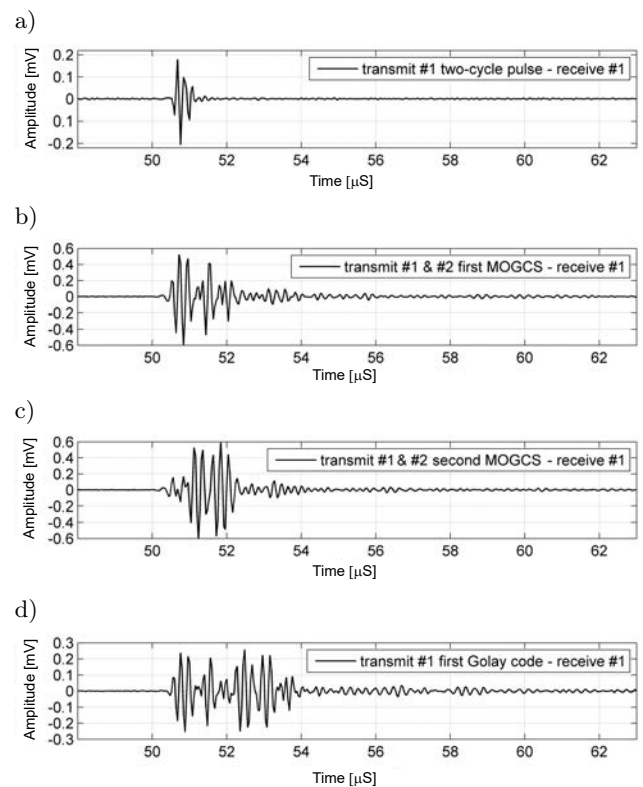


Fig. 3. RF signal reflected from a perfect reflector for the short pulse transmission (a); the MOGCS echo being a superposition of the codes  $A_1$  and  $B_1$  transmitted by the elements  $\#1$  and  $\#2$ , respectively (b); the MOGCS echo being a superposition of the codes  $A_2$  and  $B_2$  transmitted by the elements  $\#1$  and  $\#2$ , respectively (c); a first sequence from the pair of CGCS  $A_1$  transmitted and received by the element  $\#1$  (d). All echoes were detected by the element  $\#1$ .

Specifically, the short pulse echo is shown in Fig. 3a. The RF echoes recorded by the element  $\#1$  being a superposition of the 16-bits long MOGCS codes  $A_1$  and  $B_1$ ,  $A_2$  and  $B_2$  are shown in Figs 3b and 3c, respectively. Finally, a first sequence from the pair of conventional CGCS code  $A_1$  is shown in Fig. 3d. In the case of CGCS the codes  $A_1$  and  $A_2$  were transmitted successfully by the element  $\#1$  which was also used for the detection of the reflected signals.

In Fig. 4 the comparison of the signals envelopes reflected from the brass plate (see Fig. 3) are shown. In the case of MOGCS and CGCS the signals were compressed prior to the envelope detection. The half maximum (measured at the  $-6$  dB level) time duration of the envelopes for both MOGCS and CGCS were approximately equal  $0.34 \mu\text{s}$ . The corresponding value for the short pulse was  $0.42 \mu\text{s}$ . The above values of the time duration expressed in units of spatial distance were  $0.52 \text{ mm}$  for coded excitation (MOGCS and CGCS) and  $0.65 \text{ mm}$  for the short two-cycle pulse. The time duration of the envelopes measured at the  $0.1$  level ( $-20$  dB) was  $0.88 \mu\text{s}$  for the MOGCS,  $1.0 \mu\text{s}$  for the CGCS and  $0.72 \mu\text{s}$  for the short pulse transmis-

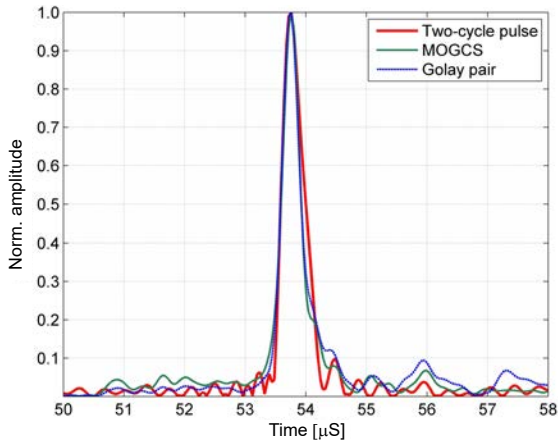


Fig. 4. Comparison of the processed RF echoes obtained from the perfect reflector using the short pulse, the MOGCS, and the CGCS transmitted signals.

sion. These corresponded to 1.36 mm for the MOGCS, 1.54 mm for the CGCS, and 1.1 mm for the short pulse transmission.

In Fig. 5 the envelopes of the RF signals collected from the nylon wire phantom are shown.

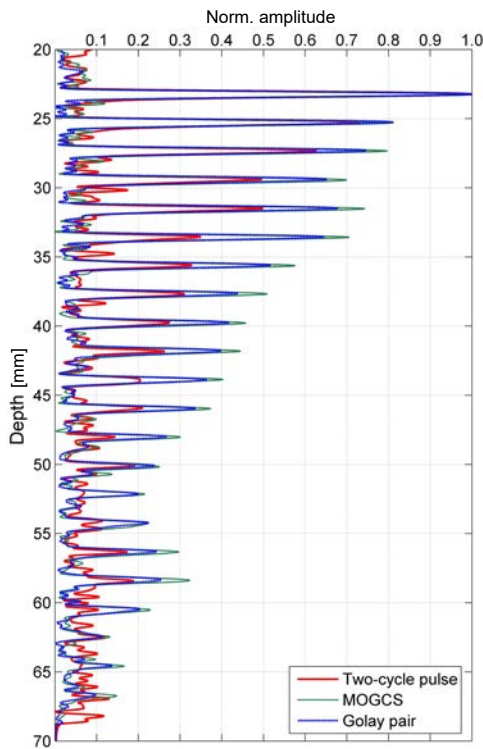


Fig. 5. Comparison of the processed RF echoes from the nylon wire phantom obtained using the short pulse, MOGCS and CGCS transmitted signals.

In the case of the MOGCS and the CGCS the signals were compressed prior to the envelope detection. To compare the efficiency of the MOGCS echoes separation the SLL at different depths was estimated and compared to those obtained for the conventional

CGCS compressed signal. The results are shown in Fig. 6. The SLL for the short pulse was also estimated for comparison. As can be seen from Fig. 6 the SLL for all types of transmission signals increases with depth. The results in Fig. 6 also demonstrates that simultaneous transmission of the the MOGCS and separation of the received echoes using compression technique do not influence significantly the SLL of the MOGCS in comparison with conventional CGCS transmitted successfully.

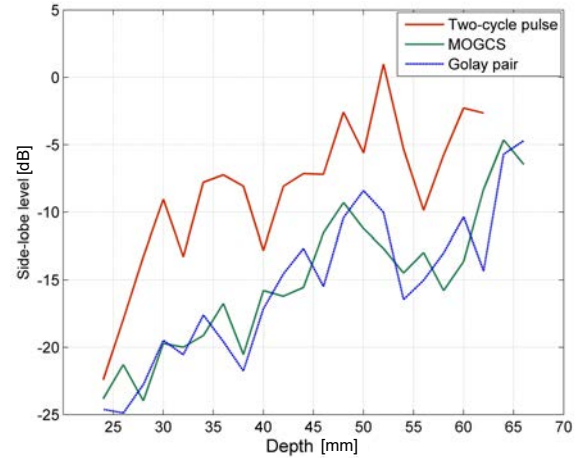


Fig. 6. The SLL vs. depth for the processed signals obtained from the wire phantom (see Fig. 5).

In Fig. 7 the received echoes (the absolute values) collected from the tissue-mimicking phantom (model 525 Danish Phantom Design) which consist of nylon

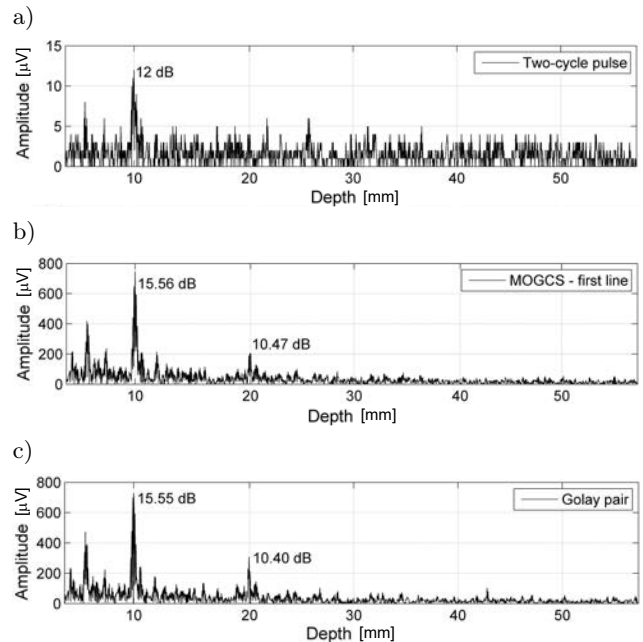


Fig. 7. Comparison of the SNR for tissue-mimicking phantom echoes obtained using the short pulse (a); the MOGCS (b); the conventional CGCS (c) transmission. The absolute values of the received echoes are shown.

filaments twisted more than one time per mm located every 10 mm axially are shown. For more objective comparison the measurements were performed without amplifying echo signal. Because of this, the imaging range was limited to only 20 mm in the case using Golay codes. The SNR value estimated (MISARIDIS, 2001) at the depth of 10 mm and 20 mm was 15.56 dB and 10.47 dB for the MOGCS and 15.55 dB and 10.40 dB for the conventional CGCS. In the case of the short two-cycle pulse only the SNR value at the depth of 10 mm could be obtained. It was equal 12 dB.

The 2D B-mode reconstructed images of the wire phantom using the MOGCS as well as CGCS and for comparison the two-cycle pulse are shown in Fig. 8. The phantom consists of 22 nylon wires arranged at angle  $10^\circ$  vertically and spaced 2 mm axially.

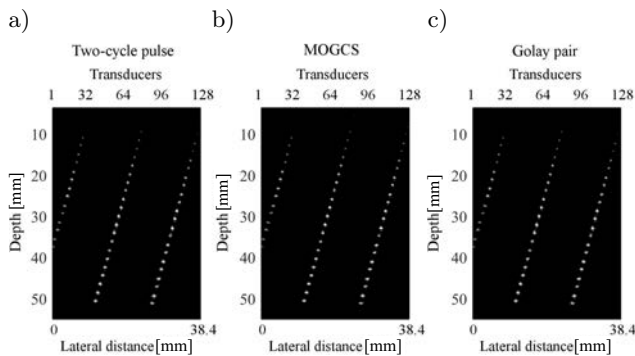


Fig. 8. Comparison of the 2D B-mode images of the wire phantom obtained using the short pulse (a); the MOGCS (b); the conventional CGCS (c) transmission.

The obtained 2D ultrasound images clearly demonstrate that image resolution is almost the same in all cases. Due to the fact that the measurements were carried out in water (no attenuation of the transmitted signal), the penetration depth is also the same. The reconstructed time for case MOGCS (Fig. 8b) decreases twice in comparison to CGCS and is the same for the two-cycle short pulse. Using MOGCS 4 or higher order, the image reconstructed time can be reduced that allows increasing frame rate proportionally (HUANG, 2005). As a result in the case of 4-th order MOGCS the four coded sequences set is transmitting by four transducers during one transmission and as a result the 4 image lines can be constructed after two transmissions. In the case of 8-th order MOGCS the eight coded sequences set is used and as a result after two transmissions the 8 image lines can be constructed.

## 5. Conclusions

In this work we compared the SNR, the SLL and axial resolution of the compressed echoes resulting from simultaneous transmission of the two sets of 16-bits long MOGCS, successful transmission of the con-

ventional CGCS pair and the short two-cycle pulse transmission. The results confirmed that simultaneous transmission of the MOGCS and separation of the combined RF echoes on the receiver side does not worsen the parameters of the signals in comparison to the conventional CGCS. At the same time, transmission of two MOGCS sets allows maintaining the axial resolution and data acquisition speed as in the case of the short pulse transmission. The frame rate can be further increased if more than two sets of the MOGCS are used. The results demonstrate the advantage of MOGCS in the modern ultrasound diagnostics compared to the conventional short pulse excitation and CGCS.

## Acknowledgments

This work was supported by National Centre for Research and Development (NCBiR) Grant No. INFOSTRATEG-I/0042/2021.

## References

1. BAE M.H. (2003), *Ultrasound imaging method and apparatus using orthogonal Golay codes*, U.S. Patent US6638227B2.
2. BAE M.-H., LEE W.-Y., JEONG M.-K., KWON S.-J. (2002), Orthogonal Golay code based ultrasonic imaging without reducing frame rate, [in:] *2002 IEEE Ultrasonic Symposium, 2002. Proceedings*, **2**: 1705–1708, doi: 10.1109/ULTSYM.2002.1192625.
3. CHIAO R.Y., THOMAS L.J. (2000), Synthetic transmit aperture imaging using orthogonal Golay coded excitation, [in:] *2000 IEEE Ultrasonics Symposium. Proceedings. An International Symposium (Cat. No. 00CH37121)*, **2**: 1677–1680, doi: 10.1109/ULTSYM.2000.921644.
4. GOLAY M. (1961), Complementary series, *IRE Transactions on Information Theory*, **7**(2): 82–87, doi: 10.1109/TIT.1961.1057620.
5. HUANG X. (2005), Simple implementation of mutually orthogonal complementary sets of sequences, [in:] *2005 International Symposium on Intelligent Signal Processing and Communication Systems*, pp. 369–372, doi: 10.1109/ISPACS.2005.1595423.
6. KIM B.-H., SONG T.-K. (2003), Multiple transmit focusing using modified orthogonal Golay codes for small scale systems, [in:] *IEEE Symposium on Ultrasonics*, pp. 1574–1577, doi: 10.1109/ULTSYM.2003.1293208.
7. KUMRU Y., KOYMEN H. (2018), Beam coding with orthogonal complementary Golay codes for signal-to-noise ratio improvement in ultrasound mammography, *The Journal of the Acoustical Society of America*, **144**(3): 1888–1888, doi: 10.1121/1.5068277.

8. MISARIDIS T. (2001), *Ultrasound imaging using coded signals*, Center for Fast Ultrasound Imaging Technical University of Denmark, PhD Thesis, 194 pages.
9. NOWICKI A., SECOMSKI W., LITNIEWSKI J., TROTS I. (2003), On the application of signal compression using Golay's codes sequences in ultrasound diagnostic, *Archives of Acoustics*, **28**(4): 313–324.
10. PENG H., HAN X., LU J. (2006), Study on application of complementary Golay code into high frame rate ultrasonic imaging system, *Ultrasonics*, **44**: e93–e96.
11. TIAN L., LU X., XU C., LI Y. (2021), New mutually orthogonal complementary sets with non-power-of-two lengths, *IEEE Signal Processing Letters*, **28**: 359–363, doi: 10.1109/LSP.2021.3054565.
12. TROTS I. (2015), Mutually orthogonal Golay complementary sequences in synthetic aperture imaging systems, *Archives of Acoustics*, **40**(2): 283–289, doi: 10.1515/aoa-2015-0031.
13. TROTS I., NOWICKI A., SECOMSKI W., LITNIEWSKI J. (2004), Golay sequences – side-lobe canceling codes for ultrasonography, *Archives of Acoustics*, **29**(1): 87–97.
14. TROTS I., TASINKEVYCH Y., NOWICKI A. (2015), Orthogonal Golay codes with local beam pattern correction in ultrasonic imaging, *IEEE Signal Processing Letters*, **22**(10): 1681–1684, doi: 10.1109/LSP.2015.2423619.
15. TROTS I., TASINKEVYCH Y., NOWICKI A., LEWANDOWSKI M. (2011), Golay coded sequences in synthetic aperture imaging systems, *Archives of Acoustics*, **36**(4): 913–926.
16. TSENG C.C., LIU C.L. (1972), Complementary sets of sequences, *IEEE Transactions on Information Theory*, **18**: 644–652, doi: 10.1109/TIT.1972.1054860.
17. WU S.-W., CHEN C.-Y., LIU Z. (2021), How to construct mutually orthogonal complementary sets with non-power-of two lengths?, *IEEE Transactions on Information Theory*, **67**(6): 3464–3472, doi: 10.1109/TIT.2020.2980818.
18. ZHAO F., LUO J. (2018), Diverging wave compounding with spatio-temporal encoding using orthogonal Golay pairs for high frame rate imaging, *Ultrasonics*, **89**: 155–165, doi: 10.1016/j.ultras.2018.05.009.